Aging and arsenite loading control arsenic mobility from ferrihydrite-arsenite coprecipitates

(Article begins on next page)

19 October 2024

UNIVERSITÀ DEGLI STUDI DI TORINO

Aging and arsenite loading control arsenic mobility from ferrihydrite-arsenite coprecipitates

Elena Zanzo[a], Ramona Balint[a,b,*] Marco Prati[a], Luisella Celi[a], Elisabetta Barberis[a], Antonio Violante[c], Maria Martin[a]

Aging and arsenite loading control arsenic mobility from ferrihydrite-arsenite coprecipitates

Elena Zanzo[a], Ramona Balint[a,b,*] Marco Prati[a], Luisella Celi[a], Elisabetta Barberis[a], Antonio Violante[c], Maria Martin[a]

[a]Department of Agricultural, Forest and Food Sciences, Agricultural Chemistry and Pedology, University of Turin, Largo Paolo Braccini n. 2, 10095 Grugliasco (TO), Italy
[b]Geological Institute of Romania, Str. Caransebes nr. 1, Sector 1, 012271, Bucharest, Romania
[c]Department of Agriculture, University of Naples Federico II, Via Università, n. 100, 80055 Portici (Naples), Italy
*Corresponding author: R. Balint. E-mail address: ramona.balint@unito.it
Tel.: +39 0116708687; Fax: +39 0116708692.

Abstract

Iron (hydr)oxides may act as sink and source of arsenic (As) in the terrestrial and aquatic systems, therefore studying the mechanisms controlling Fe (hydr)oxide transformation under changing environmental conditions is essential for elucidating the fate of As, in terms of release, mobility and speciation. We studied the potential extraction of As(III) and As(V) from Fe-As(III) coprecipitates by different anions, commonly occurring in soil solution, and showed that their efficiency decreased in the order: phosphate > citrate > inositol hexaphosphate > chloride ≥ silicate. We provide evidence that As removal is influenced by the mineralogical and structural evolution of As-bearing ferrihydrite as a consequence of aging and increasing As loadings. These parameters promoted partial As(III) oxidation to As(V) and accumulation on short-range order Fe (hydr)oxides, due to incomplete ferrihydrite to goethite conversion. The changes in crystallinity degree and surface properties resulted in the release of different proportions of As(III) and As(V) from the aged compared to the fresh coprecipitates, through mechanisms of competition, disaggregation of Fe (hydr)oxides, or both. The tested extractants are key components of environments such as aquifers, waterlogged soils, or the rhizosphere, where aqueous As(III) is mobilized from the anoxic to oxic layer and sequestered by Fe (hydr)oxides.

Keywords: arsenic, iron, competing ion, dissolution, crystallization

1. Introduction

Arsenic (As) is a toxic element present in all natural environments. The contamination of aquifers by As is of great concern at local and global level, especially in southeast Asia where As-polluted groundwater is used both as drinking and irrigation waters [1]. The endemic As poisoning in India, Bangladesh and China is attributed to the high levels of inorganic As in well waters [1,2]. Both As(V) and As(III) may co-exist in aquatic systems and their speciation depends, besides redox conditions, on pH, ionic strength, microbial activity, organic matter, and type and availability of reactive mineral surfaces [3]. Arsenate (As(V)), in fact, strongly adsorbs onto poorly-ordered Fe and Al (hydr)oxides, while the more toxic arsenite (As(III)) bonds mainly with Fe (hydr)oxides [4-7]. The formation of Fe-As coprecipitates may occur in natural environments, particularly under anoxic conditions encountered in reducing groundwater or flooded rice fields, where dissolved Fe(II) is often present in high concentrations [1,3,8,9]. When oxidizing conditions are restored, the precipitation of Fe (hydr)oxides may effectively scavenge As from aqueous solutions, with the formation of Fe-As coprecipitates [1,10]. Apart from adsorption and coprecipitation on/with Fe (hydr)oxides, As(V) and As(III) may also form poorly soluble salts, like scorodite ($FeAsO_4 \cdot 2H_2O$) or ferric arsenate ($FeAsO_4 \cdot nH_2O$), and orpiment (As_2S_3)[10].

The stability of such minerals, in particular As(V)-containing Fe (hydr)oxides, was thoroughly investigated and their As/Fe molar ratio was indicated as a key factor controlling oxide mineralogy and crystallinity degree [11,12]. Furthermore, high As(V) loadings are known to limit the long-term stability of Fe-As(V) (hydr)oxides, since their conversion from less to more crystalline phases as a result of aging or thermal treatment is inhibited by the coprecipitation of large amounts of As(V) [7,12]. However, to the best of our knowledge, little attention has been paid to the coprecipitation of As(III) at different As(III)/Fe molar ratios and their role in the transformation of short-range order Fe-As(III) (hydr)oxides with time.

The speciation, mobility and fate of As from Fe-As precipitation products may also be significantly altered by the variation of environmental factors and interferences of dissolved organic and inorganic compounds on the association of As with Fe oxides [13]. For instance, common anions in groundwater and soil solution such as chloride, silicate, phosphate and citrate may affect the sorption/desorption of As on/from Fe-As coprecipitates [14]. Phosphate and silicate are important competitors of As(V) for binding sites, since they are all tetrahedral anions, forming inner-sphere complexes with Fe oxides [3-6,10]. An even higher capacity to displace anions from minerals than inorganic phosphate was previously attributed to inositol hexaphosphate (Ins6P) [15, 16], which is

the most abundant form of organic phosphorus in soil [17]. Another organic compound commonly present in soil is citrate, capable to dissolve Fe (hydr)oxides, form stable colloidal suspensions [18], complex Fe and compete with other anions for surface sites, potentially leading to the release of associated As [14,19,20]. This may provide an important source of contamination to waters or crops and potentially pose a risk to human health. Based on these considerations, the effects of As(V) association on metal oxide mineralogy and physical properties and subsequent extraction by competing anions have been thoroughly investigated, whereas there is a lack of knowledge regarding the fate of Fe-As(III) coprecipitates and the mobility of coprecipitated As(III) with respect to adsorbed As(III) and coprecipitated As(V). We hypothesize that also the structural properties of Fe(III)-As(III) coprecipitates and potential As release by competing anions are strongly influenced by aging and As loading. Consequently, we aim at studying these processes by: (i) analyzing the mineralogy and reactivity of fresh and aged Fe-As(III) coprecipitates with different As/Fe molar ratios; (ii) assessing As speciation and potential mobility from Fe-As(III) coprecipitates under different environmental conditions and competing anions.

2. Materials and methods

2.1. Preparation of Fe-As(III) coprecipitates

Fe-As(III) coprecipitates were formed by mixing sodium arsenite ($NaAsO_2$, Sigma-Aldrich™) with 0.1 M iron nitrate ($Fe(NO_3)_3$) to obtain 0, 0.005, 0.01 and 0.05 As/Fe molar ratios (R), in order to assess the effect of different As loadings on the mineralogical characteristics of As-bearing Fe (hydr)oxides and on the mobility of As. The solutions were brought to pH 7.0 by slowly adding 1 M NaOH, until producing reddish-brown precipitates. The suspensions were subsequently dialyzed until the electrical conductivity of the eluates was less than 5 $\mu S\ cm^{-1}$. Part of the samples was immediately subjected to analyses (t_0), either directly as suspension or after freeze-drying, while the rest was aged in suspension for one year (t_1) at ambient temperature (25±2 °C), followed by investigations similar to those performed on fresh materials. Aliquots of each suspension were centrifuged (1500 g for 15 min) and filtered (0.45 μm), and the supernatants were analyzed for As by Hydride Generating Atomic Absorption Spectroscopy (HG-AAS; Perkin Elmer FIAS 4100, Waltham, MA, U.S.A.). The results showed As concentrations below detection limit (0.25 $\mu g\ L^{-1}$) for all Fe-As(III) coprecipitates.

2.2. Mineralogical, physical and chemical analyses

The mineralogy of the Fe-As(III) coprecipitates was identified by X-ray diffraction (XRD; Philips PW1710, PANalytical B.V., Almelo, The Netherlands) with CoKα radiation filtered by a graphite monochromator at 40 kV and 160 mA. The XRD patterns were recorded in the range between 10° and 80° 2θ, with 0.02° 2θ steps at a scanning rate of 4 sec/step. The specific surface area (SSA) of the Fe-As(III) coprecipitation products was determined in duplicate by N_2 adsorption (Fison Sorptomatic 1900, Carlo Erba Instruments, Rodano, MI, Italy). The adsorption isotherms obtained were typical of microporous materials; therefore it was more appropriate to calculate the SSA of micropores (SSA_{micro}) by Dubinin equation with respect to the Brunauer-Emmett-Teller (B.E.T.) method [25,26]. The XRD and SSA_{micro} analyses were performed on the fresh and aged freeze-dried samples.

Before freeze-drying, zeta potential (ζ) was measured as a function of pH and the point of zero charge (PZC) was determined. The suspensions of fresh and aged Fe-As(III) coprecipitates were diluted and analyzed in duplicate by Laser Doppler Velocimetry coupled with Photon Correlation spectroscopy (DELSA 440, Beckman Coulter Inc., Brea, CA, U.S.A) to determine their electrophoretic mobility. The data were converted to ζ using the Smoluchowski equation [27].

Total Fe (Fe_t) and As (As_t) were determined in triplicate by complete dissolution of all coprecipitates with *aqua regia* and the resulted As/Fe molar ratios were in line with the theoretical ones (Table 1S of the Supplementary Data). Short-range order Fe (hydr)oxides were dissolved with 0.3 M ammonium oxalate at pH 3 [28] and the extracted Fe (Fe_o) and As(As_o) were analyzed. The difference between *aqua regia*- and oxalate-extractable Fe was used to estimate the fraction of high crystallinity degree Fe (hydr)oxides (Fe_c) of all Fe-As(III) precipitation products (Table 1). All solutions were analyzed by Flame Atomic Absorption Spectroscopy (F-AAS; Perkin Elmer AAnalyst 400, Waltham, MA, U.S.A.) for total Fe (detection limit – 0.1 mg L^{-1}) and by HG-AAS for total As (Table 1S). The European Reference Material CC-018 was used to ensure analytical reproducibility and the relative standard deviation (RSD) between the certified value and measured As was less than 1%.

2.3. Arsenite and arsenate release from the Fe-As(III) coprecipitates

Arsenite and arsenate release tests were carried out in duplicate with inorganic (potassium chloride - KCl, monopotassium phosphate - KH_2PO_4 and sodium metasilicate - Na_2SiO_3 from Sigma-Aldrich™) and organic ions (dipotassium inositol hexaphosphate - $C_6H_{16}K_2O_{24}P_6$ and sodium citrate - $Na_3C_6H_5O_7$ from Sigma-Aldrich™) commonly present in the soil solution. It should be noted that

metasilicate ions hydrolyze instantly to form orthosilicate ions and silicic acid molecules. Duplicate aliquots of each Fe-As(III) precipitation product (100 mg) were equilibrated in polyethylene test tubes for 8 hours with 10 mL extractant at two concentrations (0.01 M and 0.1 M) to obtain 1 and 10 mM of competitive anion per gram of coprecipitate, respectively. The final solid: solution ratio was 1:100. Since silicate easily polymerises at high concentrations, the extractions with this reagent were performed only at 0.01M. The experiments were conducted at two different pH values (4.5 and 8.5) obtained by adding 0.01 or 0.1 M HCl and 0.01 or 0.1 M NaOH, respectively. After shaking for 24 h in the dark at room temperature (25±2 °C), the samples were centrifuged (1500 g for 15 min), filtered on 0.45 μm filters and the supernatant was analyzed for As by HG-AAS.

Arsenic speciation was determined by analysing total As and As(III) (HG-ASS) and calculating As(V) concentrations as the difference between them. For the analysis of As(III) a citric acid-sodium citrate buffer was used, instead of HCl, both for sample preparation and as carrier solution in the flow-injection system [29,30]. Total Fe was also determined by F-AAS for the extractants with dissolutive mechanisms – Ins6P and citrate. The RSD for all As and Fe analyses was within 7 and 5%, respectively.

3. Results and discussion

3.1. Characterization of Fe-As(III) coprecipitates

The XRD patterns of fresh (t_0) Fe-As(III) precipitation products presented the broad peaks characteristic of poorly crystalline 2-line ferrihydrite regardless of the As/Fe molar ratio (Fig. 1A). Additionally, Figure 1B shows an increase in the crystallinity degree of t_1 with respect to t_0 samples, as indicated by the sharp peaks specific for goethite (d-spacing: 0.418, 0.245 and 0.269 nm [31]). However, these peaks became broader with growing amounts of coprecipitated As, suggesting a gradual decrease in the goethite to ferrihydrite ratio. The presence of goethite needle-like crystals was also ascertained by transmission electron microscopy in the t_1 samples with low As(III) contents (data not shown). Similarly to our results, Violante et al. (2007) have shown that As(V) coprecipitation with Fe at elevated As/Fe molar ratios limited the formation of crystalline Fe-As(V) materials and the transformation of As(V)-loaded ferrihydrite into goethite as a result of aging [24]. Moreover, As(V) adsorption onto ferrihydrite at increasing As/Fe molar ratios generated poorly crystalline materials which presented the XRD patterns characteristic of a gradual conversion from two-line ferrihydrite to a poorly crystalline ferric arsenate phase, as

revealed by Jia et al. [32]. Furthermore, Thoral et al. [33] also suggested that the presence of As(III) during Fe(II) oxidation results in the formation of amorphous phases composed of nanosized clusters.

In agreement with XRD patterns, SSA_{micro} of Fe-As(III) precipitation products was affected by As/Fe molar ratios (Table 1). Although the effect of As/Fe ratio was not statistically different for the t_0 samples, we nonetheless noticed a significant raise in the SSA_{micro} of t_1 materials ($P<0.05$), indicating that the coprecipitation of large amounts of As(III) with Fe hampered the formation of ordinate Fe (hydr)oxide structures with time. A two-way ANOVA showed, indeed, that the interaction As/Fe ratio x time significantly affected the SSA_{micro} of the coprecipitates ($P<0.01$). Additionally, we observed a higher effect of aging on the microporosity of As-free or low As-containing materials (R0 and R0.005; $P<0.01$ and 0.05, respectively), whose SSA_{micro} dropped by 32 and 19% respectively, compared to their fresh counterparts (Table 1). On the other hand, the SSA_{micro} did not significantly decrease at elevated As/Fe ratios, which supports the control of As on the formation of highly crystalline Fe (hydr)oxides, as a result of aging. These findings are in line with the results on As(V) coprecipitation with Fe obtained by Violante et al. [24], who showed that high As(V)/Fe ratios promote an increase in the SSA of aggregates and limit the structural rearrangement of Fe-As(V) precipitation products with time, with respect to the samples containing lower As/Fe ratios. Therefore, aging generally leads to the formation of more ordinate structures for pure Fe (hydr)oxides, as previously observed [11,31,34-36], while increasing amounts of As appear to favour the formation and long-term stabilization of shorter-range order Fe-As(III,V) coprecipitates.

The results of Fe extraction with *aqua regia* and ammonium oxalate (Table 1S) provided an appraisal of the influence of aging and As(III) content on the formation of high crystallinity degree Fe (hydr)oxides (Fe_c; Table 1). Both aging and As/Fe ratio significantly affected Fe_c ($P<0.001$), which increased particularly for the R0 and R0.005 samples, as previously indicated by the substantial reduction of their SSA_{micro} (Table 1). On the contrary, raising the amount of coprecipitated As(III) resulted in a progressive decrease of Fe_c fraction from 39.8 to 15.9% for the t_1 materials (Table 1), supporting the hindering effect of As(III) on the transformation of ferrihydrite into goethite. Differently from the behaviour of Fe, As extractability in ammonium oxalate was generally not significantly affected by aging (Table 1S), and the As_o/As_t fractions did not substantially change with increasing As/Fe ratios, but remained close to 1 for both fresh and aged precipitation products (Table 1). This indicates that the partial transformation of As(III)-containing Fe

(hydr)oxides from less to more crystalline phases did not effectively limit the availability of As. Only the aged R0.005 coprecipitate, which also comprised the greatest proportion of Fe_c (Table 1), released significantly lower amounts of oxalate-extractable As compared to its fresh counterpart ($P<0.05$), implying some extent of crystal incorporation for As at low As/Fe ratios. Our results suggest that an important part of coprecipitated As was probably released during the structural rearrangement of As-bearing Fe (hydr)oxides, which occurs by partial dissolution and transformation of ferrihydrite into goethite [31,34], and subsequently preferentially re-associated with the remaining or newly-formed ferrihydrite. Despite the high binding capacity of ferrihydrite for As given by the larger SSA_{micro} (Table 1) compared to goethite [3,5,6,24], we cannot exclude that minor amounts of As might have been immobilized by goethite as a result of crystal growth. Analogous results were obtained by Sørensen et al. [35] who found that heat-induced aging of trace element-containing Fe (hydr)oxides led to the expulsion and surface accumulation of most Pb and Cd, in spite of the formation of a more crystalline Fe oxide. In the medium-long term, such accumulations could promote the formation of different Fe-As phases, as previously reported by Jia et al. [32] for As(V) adsorbed on the surface of ferrihydrite, particularly at high As(V) initial concentrations.

The point of zero charge (PZC) of all Fe-As(III) coprecipitates occurred at pH values around 7.5 (Table 1), which is similar to the values obtained for Fe (hydr)oxides synthesized in the absence of As(III) (R0) and in line with those reported for pure ferrihydrite and goethite [31,37]. This suggests that neither coprecipitation of As(III) at different As/Fe molar ratios nor aging significantly affected the PZC of the Fe-As(III) precipitation products, which is different from the results on As(V) obtained by Violante et al. (2007) [24]. Unlike As(V), at the neutral pH employed for the synthesis of Fe-As(III) precipitation products, As(III) is mainly in undissociated form and hence did not affect the PZC of As-loaded ferrihydrite. In addition, the constancy of pH_{PZC} with aging suggests that the hypothesized release of As and re-association with short-range order Fe (hydr)oxides involved mainly coprecipitation mechanisms, since adsorption of As(III) would have resulted in a decrease of the pH_{PZC} [3,4,38].

3.2. Release tests

3.2.1. Release with weakly competing anions: chloride and silicate

The efficiency of KCl and sodium silicate in extracting As was relatively moderate, particularly from the Fe-As(III) coprecipitates with low As/Fe molar ratios (Figs. 2 and 3; Table 2S). Chloride was

employed to estimate the release of readily soluble As because it is considered a non-competing and nonspecific anion in solid-liquid interfacial reactions. In contrast, we expected an enhanced competition of silicate with As since both silicic acid (H_4SiO_4) and arsenous acid (H_3AsO_3) have tetrahedral structures, and dissociate at similar pH values (9.9 and 9.2, respectively [39]). However, chloride unexpectedly extracted higher fractions of As than silicate (up to 1.3 and 0.2% of total As, respectively) from the fresh precipitation products (Figs. 2 and 3), suggesting that some As was probably weakly bound or physically included in the ferrihydrite micropores, which enabled the smaller chloride ions (ionic radius 1.8 Å) to easily diffuse inside the aggregates, as opposed to the larger-sized silicate. However, the amount of As extracted with chloride drastically decreased with aging and became smaller than that extracted with silicate (Table 2S), suggesting a reduction of the aliquot of loosely or physically retained As with time. Conversely, silicate extracted similar or higher fractions of As from the t_1 compared to the t_0 precipitation products (Fig. 3) suggesting that aging resulted in further alterations, besides As bonding strength and aggregate microporosity, which influenced As mobility. As previously proposed, the partial transformation of the As-bearing Fe (hydr)oxides from less to more crystalline phases may have occurred with the release of some As and relative enrichment on ferrihydrite, possibly by encapsulation in external pores. This was particularly noticeable for the coprecipitates containing the highest As/Fe ratio (R0.05), where oversaturation of binding sites apparently rendered As more readily available for extraction compared to the As-poorer materials (Table 2S).

While higher or comparable fractions of As(III) with respect to As(V) were released by chloride from the t_1 samples (Figs. 2 and 3), the extraction of t_0 materials showed a dominance of As(V) over As(III) (Fig. 2), suggesting an enhanced oxidation of As in the micropores of the fresh samples, as a result of their larger SSA_{micro} with respect to the aged materials (Table 1). Similarly, Zhao et al. (2011) showed that adsorbed As(III) was partially converted to As(V) on the surface of ferrihydrite who played the role of catalyst, while dissolved oxygen functioned as oxidant [23]. Conversely, silicate released similar or higher fractions of As(III) compared to As(V) from both t_0 and t_1 precipitation products, supporting the steric control exerted by micropores and competition as the main As extraction mechanism.

3.2.2. Release with strongly competing anions: inorganic and organic phosphorus

The Fe-As(III) precipitation products generally released higher fractions of As after extraction with inorganic phosphate (Fig. 4) and inositol hexaphosphate (Ins6P, Fig. 5) with respect to chloride and

silicate (Figs. 2 and 3). Moreover, the efficiency of Ins6P in displacing As was lower compared to phosphate (Table 3S), despite the greater extracting potential of Ins6P with respect to inorganic phosphate [14]. This may be attributed to the microporous structure of the Fe (hydr)oxides (Table 1), which controlled the capacity of As competitors to diffuse into the aggregates. Thus, the high Ins6P steric hindrance hampered its diffusion into the micropores, limiting Ins6P-oxide interactions at the external surface [14], and consequently As release (Table 3S). Moreover, these interactions, particularly between organic phosphate and ferrihydrite, commonly result in aggregate dispersion, Fe oxide dissolution, and Fe complexation [14], which may explain the relatively high concentrations of Fe extracted in Ins6P (Table 4S), while Fe release by inorganic phosphate was negligible (data not shown). Consequently, As extraction by Ins6P from the Fe-As(III) coprecipitates was generally enhanced under the conditions which promote the formation of ferrihydrite-Ins6P complexes, namely high organic phosphorus concentrations (0.1 M) and acidic pH values (Fig. 5).

Even though the extraction mechanism of inorganic phosphate was mainly governed by competition, its efficiency in releasing As was nevertheless promoted by the same conditions as Ins6P. For all samples, the amounts of As extracted in 0.1 M phosphate were between 2 and 13 times higher with respect to the 0.01 M solution (Table 3S). Moreover, the release of As from both fresh and aged coprecipitates was more effective at pH 4.5 than at pH 8.5 (Fig. 4), because the affinity of phosphate for variable charged surfaces, such as Fe (hydr)oxides decreases at subalkaline and alkaline pH values [40]. Furthermore, previous studies have shown that the sorption of both phosphate and As(V) on different soil minerals, including Fe oxides was less effective at pH 8 compared to pH 4 [41]. Indeed, the fractions of As(V) extracted by inorganic phosphate under subalkaline conditions were predominantly higher or comparable to As(III), whereas under acidic conditions, similar or lower proportions of As(V) with respect to As(III) were released (Fig. 4). Analogously to silicate, the competitive effect of phosphate was more notable for As(V) compared to As(III), probably as a result of their similar tetrahedral structures and dissociation constants (pK_{a1}= 2.1, pK_{a2}= 7.2 and pK_{a3}= 12.3 for phosphate; pK_{a1}= 2.3, pK_{a2}= 6.8 and pK_{a3}= 11.8 for arsenate and pK_{a1}= 9.2, pK_{a2}= 12.7, pK_{a3}=13.4 for arsenite, respectively) [39]. Conversely, the speciation of As extracted by Ins6P was influenced, apart from the competition mechanism, by the dissolution of short-range order Fe (hydr)oxides and indirect As release, as suggested by the higher positive correlation between all parameters found for Fe and As(III) than for Fe and As(V) (r=0.849 and 0.378, respectively; P<0.01) (Table 5S). Indeed, Ins6P often displaced similar or higher fractions of As(III) compared to As(V), particularly from the fresh coprecipitates

(Fig. 5), as a result of the facilitated sorption of Ins6P on ferrihydrite compared to goethite and subsequent Fe dissolution [14,42]. These results indicate that oxide dissolution by Ins6P prevailed over exchange with organic phosphorus as the driving mechanism for As release.

Differently from Ins6P (Fig. 5) and chloride (Fig. 2), inorganic phosphate extracted generally smaller fractions of As from the fresh Fe-As(III) precipitation products with respect to the aged ones, particularly at the lowest phosphate concentration (0.01 M, Fig. 4). This suggests that some inorganic phosphate may have been adsorbed on the free sites of fresh ferrihydrite or included in its micropores, leading to a lower competition for As with respect to the t_1 samples, and/or that the reduction of SSA_{micro} as a result of aging did not strongly inhibit the diffusion of phosphate into the remaining micropores. This is supported by the extraction at high inorganic phosphate concentration (0.1 M), where comparable fractions of As were generally released from the t_0 and t_1 coprecipitates (Fig. 4), suggesting an improved displacement of As by the additional phosphate. This was particularly notable for the fresh and aged R0.05 precipitation products which exhibited similar SSA_{micro} (Table 1), consequently releasing analogous proportions of As (Fig. 4). In contrast, 0.1 M Ins6P extracted larger fractions of As from t_1 with respect to t_0 R0.05 samples (Fig. 5). This may be attributed to the relative accumulation of As on newly-formed or residual ferrihydrite whose transformation into goethite as a result of aging was limited by the high As loading, as indicated by the extraction in oxalate (Tables 1 and 1S). This facilitated the partial dissolution of As-rich t_1 coprecipitates, composed primarily of poorly crystalline Fe (hydr)oxides (Table 1), and consequent release of As by Ins6P. In addition, the extraction of higher fractions of As(V) compared to As(III) from the aged R0.05 coprecipitates (Fig. 5) by Ins6P indicate that some of the As released during the structural rearrangement of Fe (hydr)oxides re-accumulated and oxidized mainly at the external surface of ferrihydrite, which enabled organic phosphorus to compete with As(V).

3.2.3. Release with competing/complexing ligands: citrate

Citrate generally released higher fractions of As (Fig. 6) with respect to chloride (Fig. 2), silicate (Fig. 3) and Ins6P (Fig. 5), but lower compared to inorganic phosphate (Fig. 4). Citrate is an organic ligand with a high sorption capacity on mineral surfaces, forming strong complexes with Fe, which results in Fe (hydr)oxide dissolution or colloid stabilization [18], consequently releasing As from Fe (hydr)oxide binding sites [19,20]. Similarly to the previously discussed anions, the efficiency of citrate in extracting As was greater at elevated concentrations and acidic pH values (Table 3S), as a

result of the enhanced dissolution of the Fe-As(III) coprecipitates, indicated by the high concentrations of released Fe (Table 4S), which amounted to 11% of the total. The complexation of Fe by citrate occurred with consequent As release, as suggested by the high correlations between Fe and As at pH 4.5 and 0.1 M concentration (r=0.783 and 0.775, respectively; $P<0.01$) (Table 5S). Shi et al. [43] observed a similar pH influence on goethite dissolution and consequent control on arsenate fixation, which were attributed to the mechanisms of citrate adsorption via inner-sphere and outer-sphere complexes under mildly acidic and subalkaline conditions, respectively. Although Fe (hydr)oxides were dissolved by both citrate and Ins6P, the amounts of As released by citrate at subalkaline pH were 8-fold lower with respect to organic phosphorus (Table 3S). This could be explained by the higher stability of Ins6P compared to citrate at pH 8.5, as indicated by their acid dissociation constants (pK_{a1}= 3.1, pK_{a2}= 4.8 and pK_{a3}= 6.4 for citrate; pK_{a1-4}= 1.8, pK_{a5}= 6.3 and pK_{a6}= 9.7 for Ins6P [44,45]). Hence, under subalkaline conditions, the action of citrate appeared to be mainly superficial, as suggested by the predominant release of As(V) which probably oxidized at the external sites of the precipitation products (Fig. 6). By contrast, the prevalent As species extracted at acidic pH values was As(III), probably as a result of a more intense solubilization of Fe (hydr)oxides (Table 4S) and consequent release of coprecipitated As. This is in line with the higher correlation of Fe and As(III) compared to Fe and As(V), for all variables considered (r=0.801 and 0.537, respectively; $P<0.01$) (Table 5S). As in the case of chloride, silicate and inorganic phosphate, the fractions of As extracted by citrate were generally higher for the samples containing increasing As/Fe molar ratios (Fig. 6). The prevalence of ferrihydrite in both fresh and aged R0.05 samples (Table 1), and the relative accumulation of As on short-range order Fe (hydr)oxides during aging, enabled the analogous dissolution of t_0 and t_1 coprecipitates and the extraction of comparable portions of As.

4.   Conclusions and environmental implications

Until now, aging of As-containing Fe (hydr)oxides was thought to result in the fixation of As as a consequence of structural rearrangement into more crystalline phases. While this is confirmed for the precipitation products containing low amounts of As(III), the current research demonstrates that large fractions of As may be released from As(III)-rich Fe (hydr)oxides, which may be encountered in aquifers or soils highly contaminated with As. We have shown that As oversaturation of binding sites exerts an inhibiting effect on the crystallization process, limiting the increase of the As-Fe bonding stability during aging. These processes alter As potential availability

and subsequently control its extraction by organic and inorganic anions through competitive or dissolutive mechanisms. Indeed, while the partial transformation of As-poor ferrihydrite into goethite resulted in a lower capacity of citrate and Ins6P to dissolve the aged Fe (hydr)oxides compared to their fresh counterparts, the hampered crystallization of As-rich materials led to the release of high fractions of As. Furthermore, the contained decrease in the microporosity of aged As-rich Fe (hydr)oxides enabled the diffusion of extracting agents similarly to the fresh precipitation products. In fact, the microporous structure of the materials restricted the access of organic phosphate to the surface as a result of steric hindrance, consequently controlling the amount of displaced As. The speciation of As in solution was influenced by the mechanism of As release, either by Fe (hydr)oxide dissolution, which resulted in the extraction of mainly As(III), or by competition, which was controlled by the similarity of the tested anions for either As(III) or As(V). In this sense, silicate exchanged mainly with As(III), probably owing to their chemical stability at the pH values employed, compared to As(V), while phosphate predominantly displaced As(V), on the account of their tetrahedral structure and similar dissociation constants. The prevalent release of As(V) by chloride from the fresh materials indicated a partial oxidation of labile-bound As(III) on the surface or in the micropores of ferrihydrite. Moreover, the extraction of relatively high fractions of As by this non-competing anion points out the potential increase in As availability in environments where Fe-As(III) coprecipitates might form, even in the absence of competitors. Furthermore, the cyclical changes in Fe (hydr)oxide crystallinity degree in soils under alternating reducing and oxidizing conditions [46,47], which was previously shown to control the release of some metallic elements (e.g., Cu, Pb, Zn) [47,48], may also influence the mobility of As. It is therefore necessary to further investigate the behaviour of As-bearing Fe (hydr)oxides under changing environmental conditions to elucidate the fate of As in terrestrial and aquatic environments.

Acknowledgements

Figure captions and table legends

Fig. 1. Powder X-ray diffraction patterns of fresh (A) and aged (B) Fe-As(III) coprecipitates. The d-spacings shown for aged Fe-As(III) coprecipitates (B) are represented in nm.

Fig. 2. Fractions of As(III) (mesh) and As(V) (diagonal lines) extracted in KCl (0.01 M and 0.1 M) at pH 4.5 and 8.5 from fresh (in white) and aged (in grey) Fe-As(III) coprecipitates. Note the break in As concentration axis. Error bars represent standard deviations.

Fig. 3. Fractions of As(III) (mesh) and As(V) (diagonal lines) extracted in silicate (0.01 M) at pH 4.5 and 8.5 from fresh (in white) and aged (in grey) Fe-As(III) coprecipitates. Error bars represent standard deviations.

Fig. 4. Fractions of As(III) (mesh) and As(V) (diagonal lines) extracted in phosphate (0.01 M and 0.1 M) at pH 4.5 and 8.5 from fresh (in white) and aged (in grey) Fe-As(III) coprecipitates. Note the different scales for As concentration axis. Error bars represent standard deviations.

Fig. 5. Fractions of As(III) (mesh) and As(V) (diagonal lines) extracted in inositol hexaphosphate (0.01 M and 0.1 M) at pH 4.5 and 8.5 from fresh (in white) and aged (in grey) Fe-As(III) coprecipitates. Note the different scales for As concentration axis and the break for pH 4.5. Error bars represent standard deviations.

Fig. 6. Fractions of As(III) (mesh) and As(V) (diagonal lines) extracted in citrate (0.01 M and 0.1 M) at pH 4.5 and 8.5 from fresh (in white) and aged (in grey) Fe-As(III) coprecipitates. Note the different scales for As concentration axis and the break for pH 4.5. Error bars represent standard deviations.

Table 1. Selected physical and chemical properties of the fresh (t_0) and aged (t_1) Fe-As(III) coprecipitates (± standard deviation)

References

[1] M. Martin, A. Violante, E. Barberis, Fate of arsenite and arsenate in flooded and not flooded soils of southwest Bangladesh irrigated with arsenic contaminated water, J. Environ. Sci. Health Part A-Toxic/Hazard. Subst. Environ. Eng., 42 (2007) 1775-1783.

[2] M. Martin, E. Bonifacio, K.M.J. Hossain, S.M.I. Huq, E. Barberis, Arsenic fixation and mobilization in the soils of the Ganges and Meghna floodplains. Impact of pedoenvironmental properties, Geoderma, 228-229 (2013) 132-141.

[3] P.L. Smedley, D.G. Kinniburgh, A review of the source, behaviour and distribution of arsenic in natural waters, Appl. Geochem., 17 (2002) 517-568.

[4] S. Goldberg, C.T. Johnston, Mechanisms of arsenic adsorption on amorphous oxides evaluated using macroscopic measurements, vibrational spectroscopy, and surface complexation modeling, J. Colloid Interface Sci., 234 (2001) 204-216.

[5] M. Martin, A. Violante, F. Ajmone-Marsan, E. Barberis, Surface interactions of arsenite and arsenate on soil colloids, Soil Sci. Soc. Am. J., 78 (2014) 157-170.

[6] M. Komárek, A. Vaněk, V. Ettler, Chemical stabilization of metals and arsenic in contaminated soils using oxides: A review, Environ. Pollut., 172 (2013) 9-22.

[7] A. Violante, M. Ricciardella, S. Del Gaudio, M. Pigna, Coprecipitation of arsenate with metal oxides: nature, mineralogy, and reactivity of aluminum precipitates, Environ. Sci. Technol., 40 (2006) 4961-4967.

[8] L.C. Roberts, S.J. Hug, A. Voegelin, J. Dittmar, R. Kretzschmar, B. Wehrli, G.C. Saha, A.B.M. Badruzzaman, M.A. Ali, Arsenic dynamics in porewater of an intermittently irrigated paddy field in Bangladesh, Environ. Sci. Technol., 45 (2011) 971-976.

[9] M. Martin, R. Ferdousi, K.M.J. Hossain, E. Barberis, Arsenic from Groundwater to Paddy Fields in Bangladesh: Solid-Liquid Partition, Sorption and Mobility, Water Air and Soil Pollution, 212 (2010) 27-36.

[10] H. Cheng, Y. Hu, J. Luo, B. Xu, J. Zhao, Geochemical processes controlling fate and transport of arsenic in acid mine drainage (AMD) and natural systems, J. Hazard. Mater., 165 (2009) 13-26.

[11] Z. Wang, D. Xiao, R.T. Bush, J. Liu, Coprecipitated arsenate inhibits thermal transformation of 2-line ferrihydrite: Implications for long-term stability of ferrihydrite, Chemosphere, 122 (2015) 88-93.

[12] J. Song, S.-Y. Jia, B. Yu, S.-H. Wu, X. Han, Formation of iron (hydr)oxides during the abiotic oxidation of Fe(II) in the presence of arsenate, J. Hazard. Mater., 294 (2015) 70-79.

[13] A. Fritzsche, T. Rennert, K.U. Totsche, Arsenic strongly associates with ferrihydrite colloids formed in a soil effluent, Environ. Pollut., 159 (2011) 1398-1405.

[14] D. Mohapatra, P. Singh, W. Zhang, P. Pullammanappallil, The effect of citrate, oxalate, acetate, silicate and phosphate on stability of synthetic arsenic-loaded ferrihydrite and Al-ferrihydrite, J. Hazard. Mater., 124 (2005) 95-100.

[15] L. Celi, G. De Luca, E. Barberis, Effects of interaction of organic and inorganic P with ferrihydrite and kaolinite-iron oxide systems on iron release, Soil Sci., 168 (2003) 479-488.

[16] C. Giaveno, L. Celi, R.M. Aveiro Cessa, M. Prati, E. Bonifacio, E. Barberis, Interaction of organic phosphorus with clays extracted from oxisols, Soil Sci., 173 (2008) 694-706.

[17] B.L. Turner, I.D. McKelvie, A novel technique for the pre-concentration and extraction of inositol hexakisphosphate from soil extracts with determination by phosphorus-31 Nuclear Magnetic Resonance, J. Environ. Qual., 31 (2002) 466-470.

[18] J. Braunschweig, C. Klier, C. Schroeder, M. Haendel, J. Bosch, K.U. Totsche, R.U. Meckenstock, Citrate influences microbial Fe hydroxide reduction via a dissolution disaggregation mechanism, Geochim. Cosmochim. Acta, 139 (2014) 434-446.

[19] A.G. Caporale, P. Punamiya, M. Pigna, A. Violante, D. Sarkar, Effect of particle size of drinking-water treatment residuals on the sorption of arsenic in the presence of competing ions, J. Hazard. Mater., 260 (2013) 644-651.

[20] J. Zhu, M. Pigna, V. Cozzolino, A.G. Caporale, A. Violante, Sorption of arsenite and arsenate on ferrihydrite: Effect of organic and inorganic ligands, J. Hazard. Mater., 189 (2011) 564-571.

[21] Q. Liang, D. Zhao, Immobilization of arsenate in a sandy loam soil using starch-stabilized magnetite nanoparticles, J. Hazard. Mater., 271 (2014) 16-23.

[22] T. Tuutijärvi, J. Lu, M. Sillanpää, G. Chen, As(V) adsorption on maghemite nanoparticles, J. Hazard. Mater., 166 (2009) 1415-1420.

[23] Z. Zhao, Y. Jia, L. Xu, S. Zhao, Adsorption and heterogeneous oxidation of As(III) on ferrihydrite, Water Res., 45 (2011) 6496-6504.

[24] A. Violante, S.D. Gaudio, M. Pigna, M. Ricciardella, D. Banerjee, Coprecipitation of arsenate with metal oxides. 2. Nature, mineralogy, and reactivity of iron(III) precipitates, Environ. Sci. Technol., 41 (2007) 8275-8280.

[25] ISO, Standard 9277:2010, Determination of the specific surface area of solids by gas adsorption - BET method, second ed., Geneve, 2012.

[26] J. Rouquerol, P. Llewellyn, F. Rouquerol, Is the BET equation applicable to microporous adsorbents?, in: P.L. Llewellyn, F. Rodriquez-Reinoso, J. Rouqerol, N. Seaton (Eds.), Studies in Surface Science and Catalysis, Elsevier, Amsterdam, 2007, pp. 49-56.

[27] R.J. Hunter, Zeta potential in colloid science: principles and applications, Academic Press, London, 1981.

[28] U. Schwertmann, R.M. Cornell, Iron oxides in the laboratory: preparation and characterization, second ed., Wiley-VCH, Weinheim, New York, 2000.

[29] R.K. Anderson, M. Thompson, E. Culbard, Selective reduction of arsenic species by continuous hydride generation. Part II. Validation of methods for application to natural waters, Analyst, 111 (1986) 1153-1158.

[30] J. Carlos González, I. Lavilla, C. Bendicho, Evaluation of non-chromatographic approaches for speciation of extractable As(III) and As(V) in environmental solid samples by FI-HGAAS, Talanta, 59 (2003) 525-534.

[31] R.M. Cornell, U. Schwertmann, The iron oxides: structure, properties, reactions, occurrences and uses, second edition, Wiley-VCH, Weinheim, 2003.

[32] Y. Jia, L. Xu, Z. Fang, G.P. Demopoulos, Observation of surface precipitation of arsenate on ferrihydrite, Environ. Sci. Technol., 40 (2006) 3248-3253.

[33] S. Thoral, J. Rose, J.M. Garnier, A. van Geen, P. Refait, A. Traverse, E. Fonda, D. Nahon, J.Y. Bottero, XAS study of iron and arsenic speciation during Fe(II) oxidation in the presence of As(III), Environ. Sci. Technol., 39 (2005) 9478-9485.

[34] S. Das, M.J. Hendry, J. Essilfie-Dughan, Transformation of two-line ferrihydrite to goethite and hematite as a function of pH and temperature, Environ. Sci. Technol., 45 (2011) 268-275.

[35] M.A. Sørensen, M.M. Stackpoole, A.I. Frenkel, R.K. Bordia, G.V. Korshin, T.H. Christensen, Aging of iron (hydr)oxides by heat treatment and effects on heavy metal binding, Environ. Sci. Technol., 34 (2000) 3991-4000.

[36] N. Yee, S. Shaw, L.G. Benning, T.H. Nguyen, The rate of ferrihydrite transformation to goethite via the Fe(II) pathway, Am. Miner., 91 (2006) 92-96.

[37] M. Kosmulski, pH-dependent surface charging and points of zero charge. IV. Update and new approach, J. Colloid Interface Sci., 337 (2009) 439-448.

[38] A. Jain, K.P. Raven, R.H. Loeppert, Arsenite and arsenate adsorption on ferrihydrite: surface charge reduction and net OH^- release stoichiometry, Environ. Sci. Technol., 33 (1999) 1179-1184.

[39] D.D. Perrin, Ionisation constants of inorganic acids and bases in aqueous solution, second ed., Pergamon, New York, 1982.

[40] W.L. Lindsay, Chemical equilibria in soils, John Wiley and Sons Ltd., Chichester, Sussex, 1979.

[41] A. Violante, M. Pigna, Competitive sorption of arsenate and phosphate on different clay minerals and soils, Soil Sci. Soc. Am. J., 66 (2002) 1788-1796.

[42] L. Celi, S. Lamacchia, F. Ajmone-Marsan, E. Barberis, Interaction of inositol hexaphosphate on clays: Adsorption and charging phenomena, Soil Sci., 164 (1999) 574-585.

[43] R. Shi, Y. Jia, C. Wang, S. Yao, Mechanism of arsenate mobilization from goethite by aliphatic carboxylic acid, J. Hazard. Mater., 163 (2009) 1129-1133.

[44] E.P. Serjeant, B. Dempsey, Ionisation constants of organic acids in aqueous solution, Pergamon, New York, 1979.

[45] D.J. Cosgrove, G.C.J. Irving, Inositol phosphates: their chemistry, biochemistry, and physiology, Elsevier, Amsterdam, 1980.

[46] R. Balint, C. Orbeci, G. Nechifor, M. Plesca, F. Ajmone-Marsan, Effect of redox conditions on the crystallinity of Fe oxides in soil, Rev. Chim., 64 (2013) 1218-1223.

[47] R. Balint, D. Said-Pullicino, F. Ajmone-Marsan, Copper dynamics under alternating redox conditions is influenced by soil properties and contamination source, J. Contam. Hydrol., 173 (2015) 83-91.

[48] R. Balint, G. Nechifor, F. Ajmone-Marsan, Leaching potential of metallic elements from contaminated soils under anoxia, Environ. Sci.-Process Impacts, 16 (2014) 211-219.

Table 2. Selected physical and chemical properties of the fresh (t_0) and aged (t_1) Fe-As(III) coprecipitates.

As/Fe molar ratio	Fresh/ aged	SSA_{micro} [a] $m^2\,g^{-1}$	pH_{PZC} [b]	As_o/As_t [c]	Fe_o/Fe_t
R0	t_0	306 ± 0.1	6.6	-	0.97
	t_1	208 ± 14.2	7.5	-	0.66
R0.005	t_0	314 ± 7.7	7.4	0.97	0.96
	t_1	253 ± 9.3	7.5	0.85	0.60
R0.01	t_0	316 ± 0.1	7.3	0.92	0.98
	t_1	281 ± 22.5	7.2	0.96	0.72
R0.05	t_0	344± 51.3	7.7	0.91	0.98
	t_1	340 ± 36.4	7.3	0.91	0.84

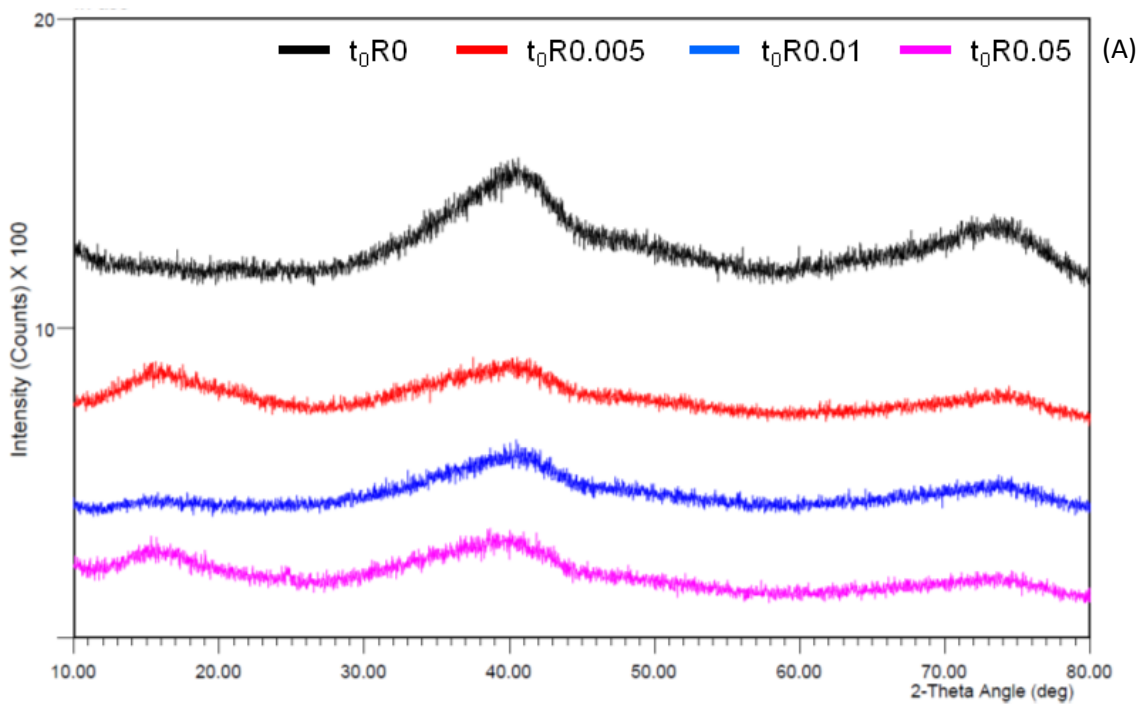[a] Specific Surface Area of micropores

[b] pH value for the Point of Zero Charge

[c] Fraction of ammonium oxalate- to aqua regia-extractable element

Table 2. Total As (nmoles g^{-1}) extracted by 0.01 and 0.1 M chloride and 0.01 M silicate from the fresh (t_0) and aged (t_1) Fe-As(III) coprecipitates, at pH 4.5 and 8.5

	Extractant		Fe-As(III) coprecipitate			
	Concentration M L^{-1}	pH	Fresh/ aged	R0.005	R0.01	R0.05
KCl	0.01	4.5	t_0	*u.d.l.*[a]	150.8 ± 9.4	2045.5 ± 37.8
			t_1	*u.d.l.*	10.3 ± 3.4	447.1 ± 0.0
		8.5	t_0	7.7 ± 1.4	399.1 ± 30.2	6098.2 ± 365.7
			t_1	*u.d.l.*	*u.d.l.*	99.1 ± 11.7
	0.1	4.5	t_0	8.7 ± 0.9	491.2 ± 43.4	3400.3 ± 184.0
			t_1	*u.d.l.*	10.7 ± 2.2	504.5 ± 0.0
		8.5	t_0	7.0 ± 0.5	401.1 ± 21.7	1660.1 ± 191.1
			t_1	*u.d.l.*	*u.d.l.*	157.8 ± 7.8
Na₂SiO₃	0.01	4.5	t_0	0.9 ± 0.1	3.3 ± 0.1	887.8 ± 0.3
			t_1	0.9 ± 0.0	34.1 ± 0.7	1072.2 ± 45.1
		8.5	t_0	1.4 ±0.0	2.7 ± 0.1	623.3 ± 18.5
			t_1	1.7 ± 0.1	22.1 ± 1.0	594.6 ± 67.9

[a] under detection limit

Figure legend: t₀R0, t₀R0.005, t₀R0.01, t₀R0.05 (A)

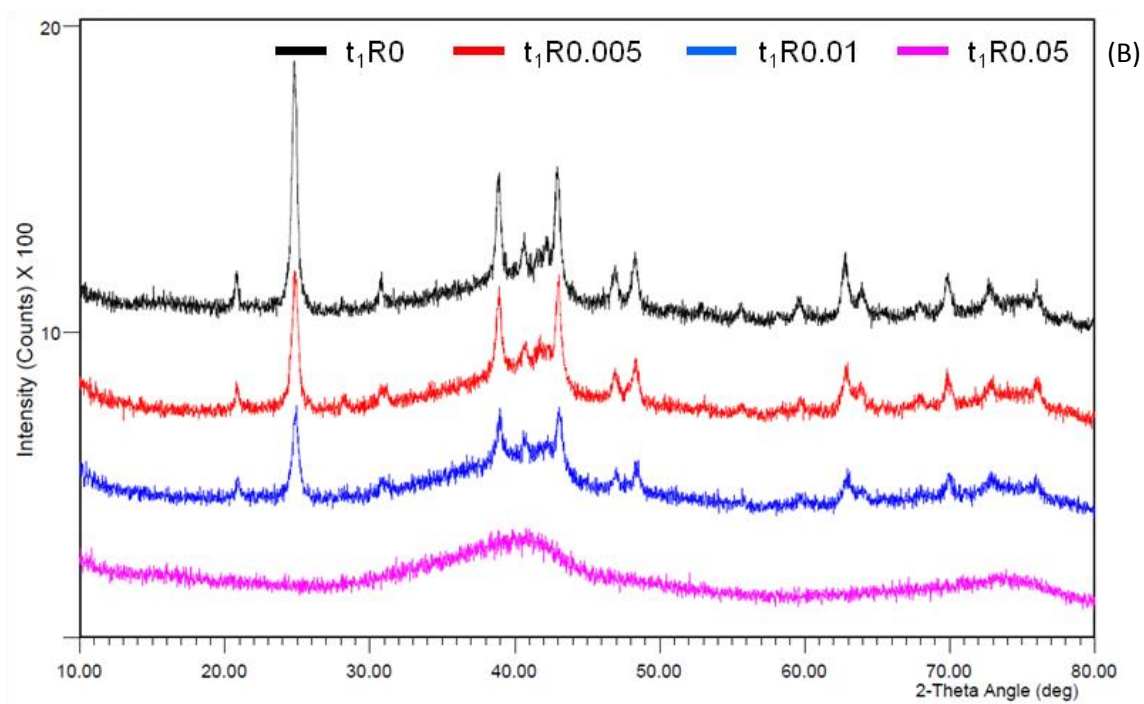Y-axis: Intensity (Counts) X 100

X-axis: 2-Theta Angle (deg)

Fig. 1. Powder X-ray diffraction patterns of fresh (A) and aged (B) Fe-As(III) coprecipitates.
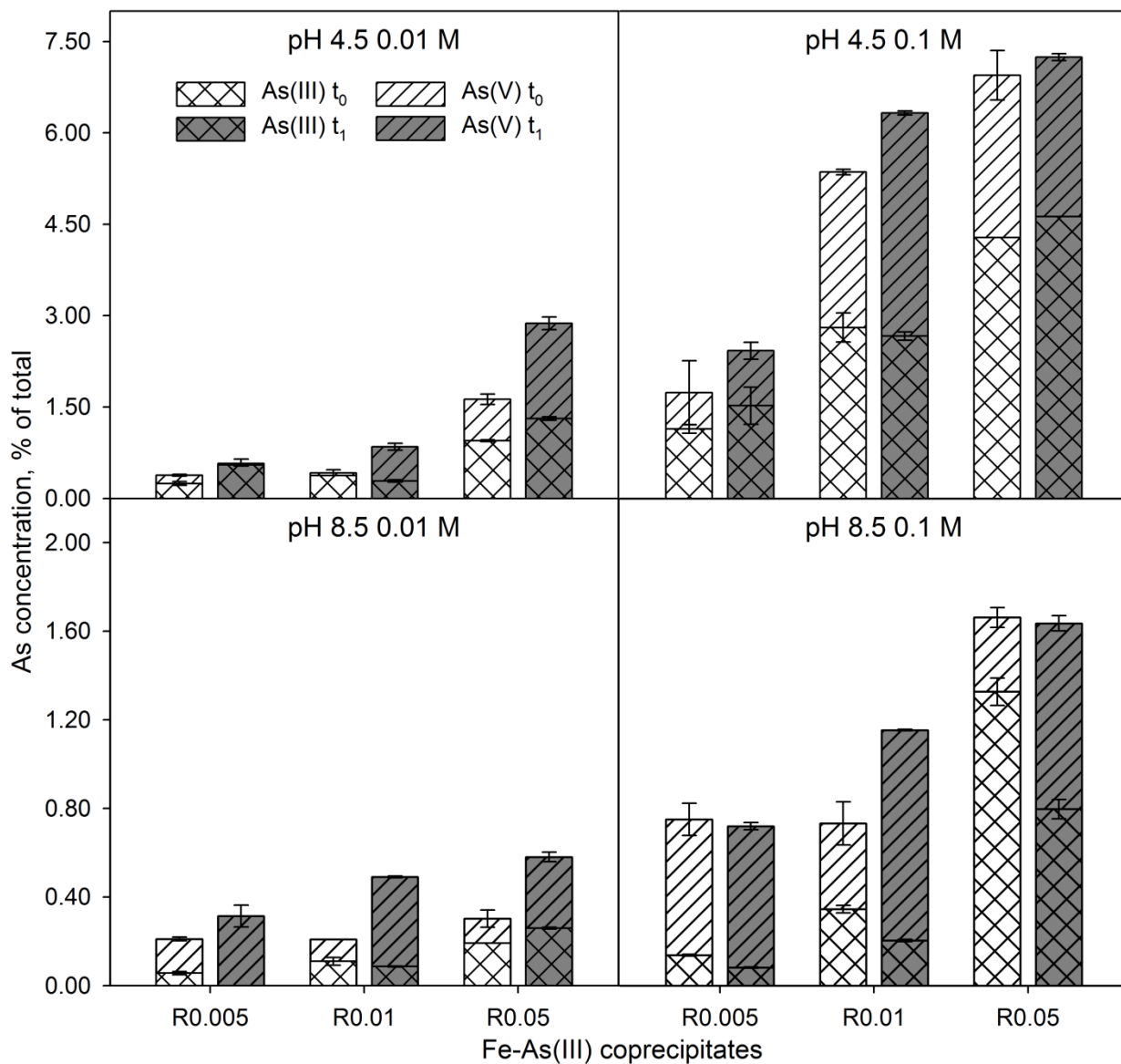
Fig. 2. Fractions of As(III) (mesh) and As(V) (diagonal lines) extracted in phosphate (0.01 M and 0.1 M) at pH 4.5 and 8.5 from fresh (in white) and aged (in grey) Fe-As(III) coprecipitates. Note the different scales for As concentration axis.
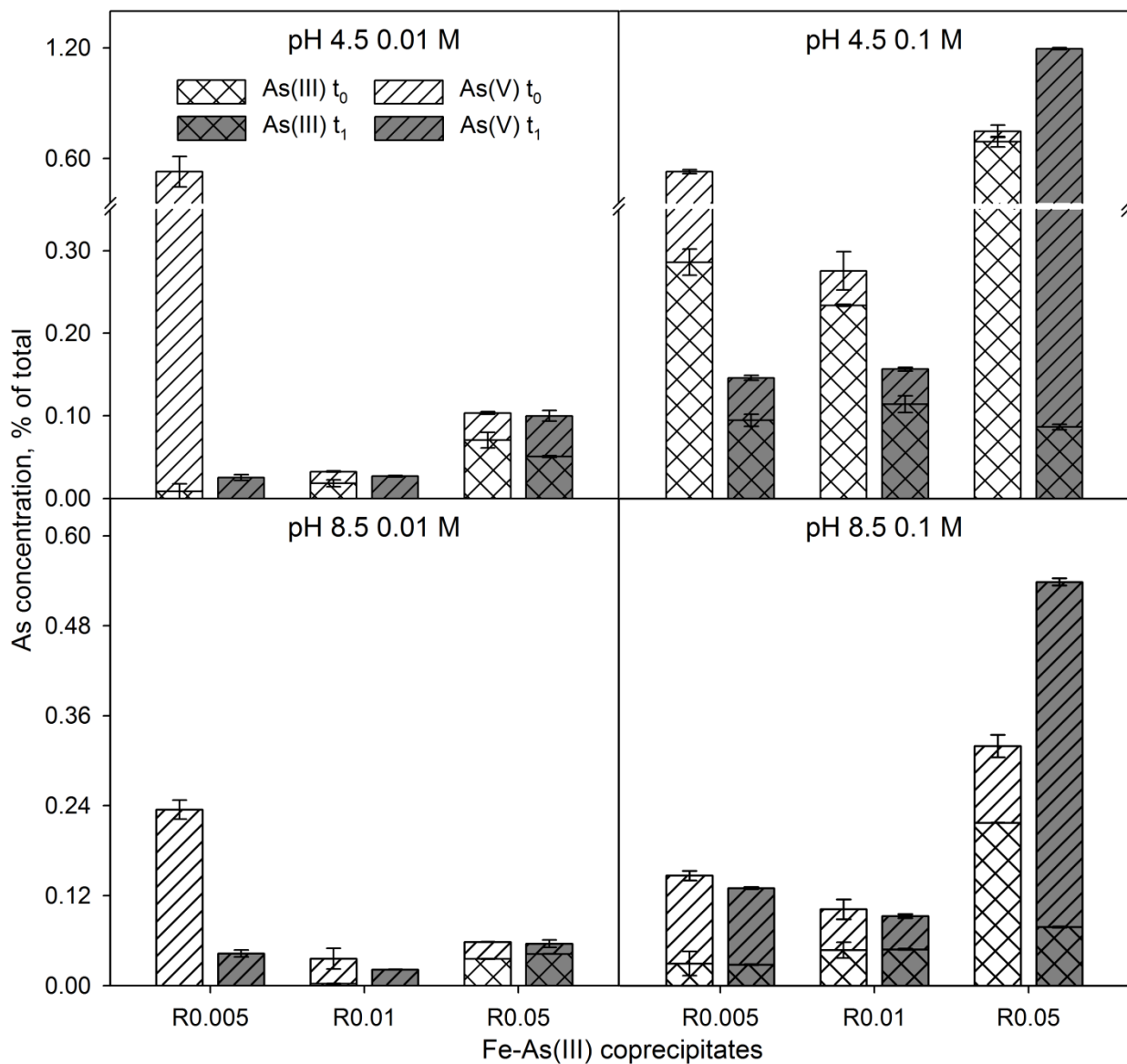
Fig. 3. Fractions of As(III) (mesh) and As(V) (diagonal lines) extracted in inositol hexaphosphate (0.01 M and 0.1 M) at pH 4.5 and 8.5 from fresh (in white) and aged (in grey) Fe-As(III) coprecipitates. Note the different scales for As concentration axis and the break for pH 4.5.
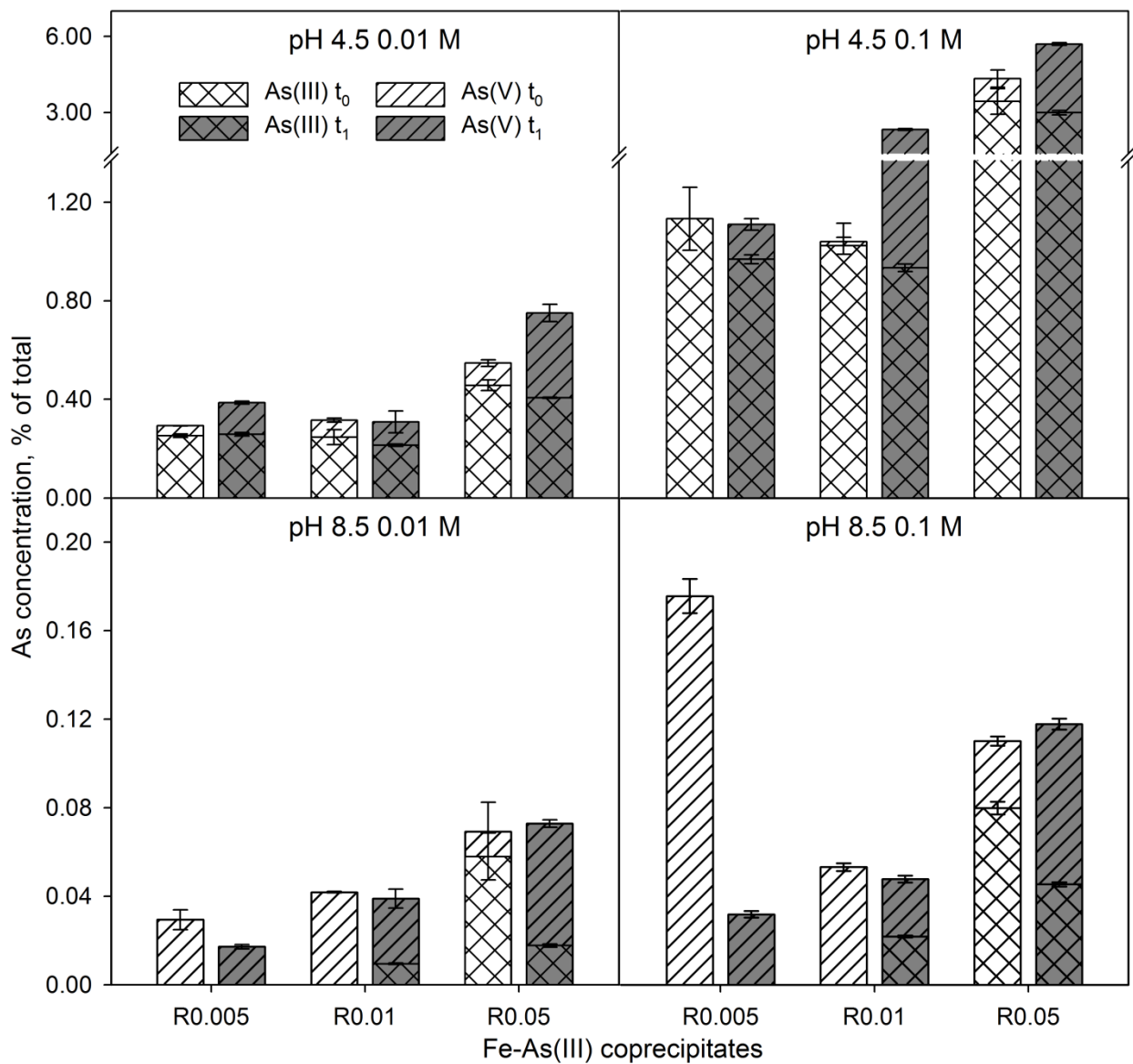
Fig. 4. Fractions of As(III) (mesh) and As(V) (diagonal lines) extracted in citrate (0.01 M and 0.1 M) at pH 4.5 and 8.5 from fresh (in white) and aged (in grey) Fe-As(III) coprecipitates. Note the different scales for As concentration axis and the break for pH 4.5.